

FREIE UNIVERSITÄT BERLIN
ADVANCED MASTER'S LABORATORY



A study into the workings of an Atomic Force Microscope
and a demonstration of its uses and limitations

Group M16

Authors:
Cian Hamilton
Leon Stone
Xiaochen Dong

Supervisor:
Dr Gaël Reecht
Course Co-Ordinator:
Prof. Dr. Martin Weinelt

November 2019

1 Abstract

The Atomic Force Microscope is a step forward in visualising ever smaller images in the atomic scale - a widespread benefit to the sciences. An exploration of the contact, noncontact with feedback, and noncontact without feedback functions gives an image of gold packing onto silicon, discusses hysteresis, drift and other errors and analyses the conical and spherical fitting of the microscope tip shape. Lastly, the relative work function between gold and highly oriented pyrolytic graphite is measured as 0.08 ± 0.02 eV which is a somewhat reasonable value since previous measurements in literature yield the work function of gold and graphite as 4.68 ± 0.03 eV[1] and 4.6 eV [2] respectively.

2 Introduction

In 1981, the Scanning Tunneling Microscope was developed by Gerd Binnig and Heinrich Rohrer [3] for which they shared the Nobel Prize in Physics in 1986 [4] [5]. This new microscope was able to resolve particles to an atomic scale. However, it had some limitations. Soon afterwards, Atomic Force Microscopy (AFM) was developed which has similar capabilities of the Scanning Tunneling Microscope but several advantages including being able to image liquids and insulating materials. AFM is often used in conjunction with STM. AFM is a very high resolution spectroscopy which can resolve images of 10^{-10} m resolution [6]. AFM can produce a 3D image which has widespread applications throughout the sciences including Biology [7], Chemistry [8], Nanoscience [10] and Electric, Magnetic and Atomic Physics[9]. This report explores the operation of the Atomic Force Microscope by measuring the topography of two different samples, gold on highly oriented pyrolytic graphite (HOPG) and gold on silicon, and by a performing voltage spectroscopy on the HOPG sample. The report aims to confirm the current understanding of the theory and application of atomic force microscopy whilst mapping gold on two different substrates and measuring the relative work function between gold and graphite.

3 Theory

3.1 The General Principles of AFM

A sharp tip is connected to a cantilever. The tip is then positioned close to the sample where it is attracted towards the sample due to forces between the tip and the sample. When the cantilever reaches a threshold distance above the sample, repulsive forces become dominant over attractive forces. The tip reaches an equilibrium distance above the sample. In atomic force microscopy, the cantilever is modelled as a linear-elastic material (i.e. it obeys Hooke's Law). A laser beam is reflected off of the top of the cantilever, and the movement of the reflected beam, measured by a photodiode, is used to determine the deflection of the beam on the cantilever. The deflection of the beam is recorded as the tip is scanned over the surface, and an image is produced of the surface with high lateral resolution. The forces involved are the short-range chemical force, the van der Waals interaction, the electrostatic force and the magnetic force. In the context of this experiment the magnetic force are neglected.

3.2 Contact Mode

In contact mode, the tip is held over the sample, and the forces between the tip and sample pull it close to the sample until they are effectively in contact. The tip is then dragged over the surface of the sample, and the deflection of the cantilever is used in a feedback circuit to keep the forces the tip-sample forces constant by changing the separation distance. The tip-sample separation distance is recorded and that is the data which is used to make the image.

3.3 Non-Contact Mode

In this mode, the cantilever oscillates near its resonance frequency due to the input of a piezo element where a small AC current is converted into the oscillating driving force[15]. The interaction between the tip and the sample occurs when the tip reaches a threshold distance. If the oscillation frequency of the cantilever is fixed, the amplitude changes. The photodiode records this change and the distance between the tip and sample surface is changed by a controller so that the preset amplitude remains constant.

3.4 Without feedback model

In this model the distance between the tip and sample kept constant[16]. And an amplitude vs. voltage curve is acquired to confirm the contact potential difference (CPD).

3.5 With feedback model

In this model the distance between the tip and sample is actively regulated, in order to obtain a tip-sample distance versus applied voltage curve.

3.6 Forces

There are several forces between the tip and sample: The short-range chemical force (repulsive and attractive forces) is described by the Lennard-Jones potential[17]:

$$U_{\text{chem}} = 4\epsilon \left[\left(\frac{\sigma_0}{r} \right)^{12} - \left(\frac{\sigma_0}{r} \right)^6 \right]$$

where ϵ is the strength of the minimal potential and σ_0 is the distance of the zero-potential.

The forces are repulsive when the distance is less than σ_0 and attractive when the distance is greater than σ_0 . The characteristics of interatomic force (van der Waals interaction) and distance are given by Figure 1.

An approximation of the van der Waals interaction between tip and surface is a sphere in front of an infinitely extended surface [18]:

$$F_{vdW} = \frac{HR}{6d^2}$$

where H is the Hamaker constant, R is the radius of the tip and d is the tip-sample distance.

Another force which needs to be taken into account is the electrostatic force, the force due to the potential difference between the sample and tip. It is given by:

$$F_{elec} = \frac{1}{2} \frac{\partial C}{\partial z} V_{eff}^2$$

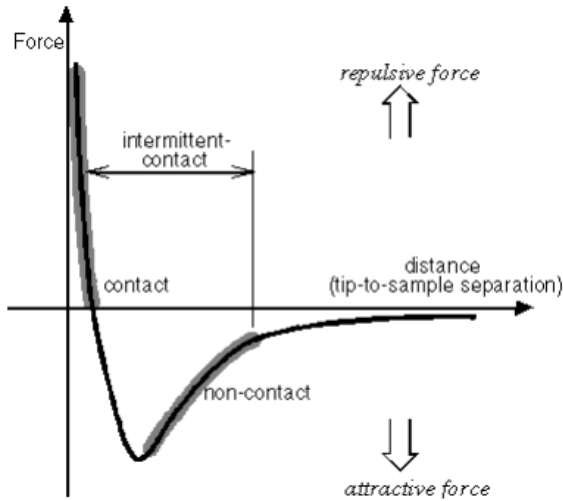


Figure 1: Interatomic force vs. distance curve

where C is the capacitance of the tip-sample capacitor and V_{eff} is the effective voltage.

The sum of these three forces is what will be affecting the tip:

$$F_{\text{total}} = F_{vdW} + F_{\text{chem}} + F_{\text{electrostatic}}$$

The equation of motion for a damped harmonic oscillator with forced oscillation is used to approximate the oscillation of the cantilever:

$$m\ddot{z} + \gamma\dot{z} + kz = F_0\cos(\omega t) + F_{\text{total}}$$

where z is the tip-sample distance, γ is the damping of the oscillation, k is the spring constant of the cantilever and $F_0\cos(\omega t)$ is the force from the oscillation made by the piezoelectric element.

The oscillation resonance frequency is:

$$\omega_0 = \sqrt{\frac{k}{m}}$$

After calculation, the interaction between tip and sample can now be included by a change in the spring constant of the cantilever and it obeys

Hooke's Law:

$$k_{\text{eff}} = k - \frac{\partial F_{\text{total}}}{\partial z}$$

The resonance frequency is changed with respect to the free resonance. An approximation of this shift $\Delta\omega_0$ is written as:

$$\Delta\omega_0 = -\frac{\omega_0}{2k} \frac{\partial F_{\text{total}}}{\partial z}$$

The contact potential difference V_{CPD} arises from the difference in work functions between the tip and the sample:

$$V_{CPD} = \frac{\Phi_{\text{sample}} - \Phi_{\text{tip}}}{e}$$

where e is the charge of an electron.

And V_{bias} is applied from outside hence:

$$V_{\text{eff}} = V_{bias} + V_{CPD}$$

4 Setup and Methodology

The Non Contact method is used to image two samples in this experiment. A typical AFM consists of a cantilever with a small tip at the free end, a laser, a 4-quadrant photodiode and a scanner as seen in figure. This is the same setup at this experiment. 2.

4.1 General

With the help of our lab assistant, we first carefully installed a new cantilever to the AFM head, and applied glue to hold it firmly in place. The glue is conductive to allow a potential difference to be applied between the tip and sample, for the voltage spectroscopy later in the experiment

Once the glue had dried, we aligned the laser so that it was reflecting off of the midpoint of cantilever. We did this by adjusting the path of the laser and observing the different diffraction patterns that were formed by the different parts of the cantilever chip.

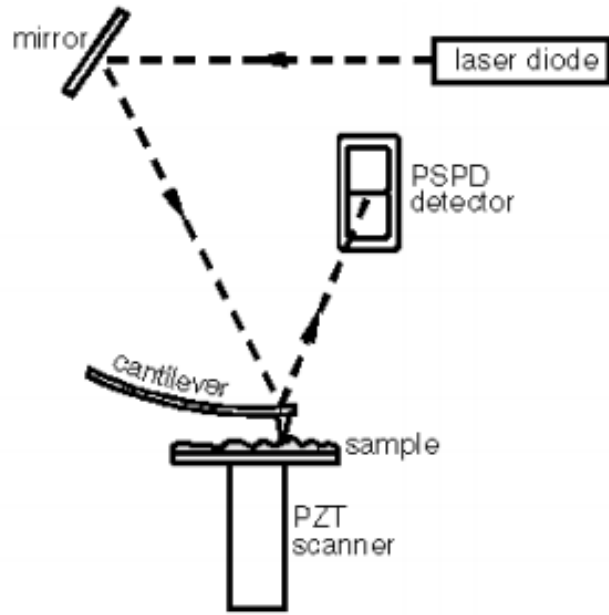


Figure 2: The beam-bounce detection scheme

Next, we aligned the photodiode so that as much as possible of the laser beam reflected from the cantilever would be picked up by the photodiode. We did this by manoeuvring the photodiode to maximise the optical power.

4.2 Sample A

We scanned sample A at different scales, from $1 (\mu\text{m})^2$, to $16 (\mu\text{m})^2$.

We performed voltage spectroscopy to measure the contact potential difference (CPD) between graphite and the tip, and gold and the tip.

This was performed by holding the tip directly over a gold portion of the sample and ramping the voltage through -2 V to +2 V. While the voltage was changing we kept a constant distance between the tip and sample, and determining the deflection of the cantilever by measuring the photodiode's output.

We did this process at 10 different points on gold portions of the sample, and repeated this for graphite.

To obtain measurements which would later allow us to determine the shape of the tip, we did a similar process to the other voltage spectroscopy, although this time it did not matter which material that the tip was over. We ramped the voltage from -9 V through to +9 V, and the tip was regulated to keep oscillation amplitude constant. We measured the tip height as a function of applied potential difference.

4.3 Sample B

Since the equipment is extremely sensitive, and as the switching of the samples involves removing the AFM head, we repeated the alignment of the laserbeam on the cantilever, and the reflected beam on the photodiode.

For sample B we scanned the surface at different scales so we could determine the size of polystyrene balls which were part of the sample before they were removed. Since the balls were on the scale of a few micrometers in size, we scanned areas of $36 \text{ } (\mu\text{m})^2$ to $2500 \text{ } (\mu\text{m})^2$.

5 Results

A Lorentz curve fit yields the resonance frequency of the tip.

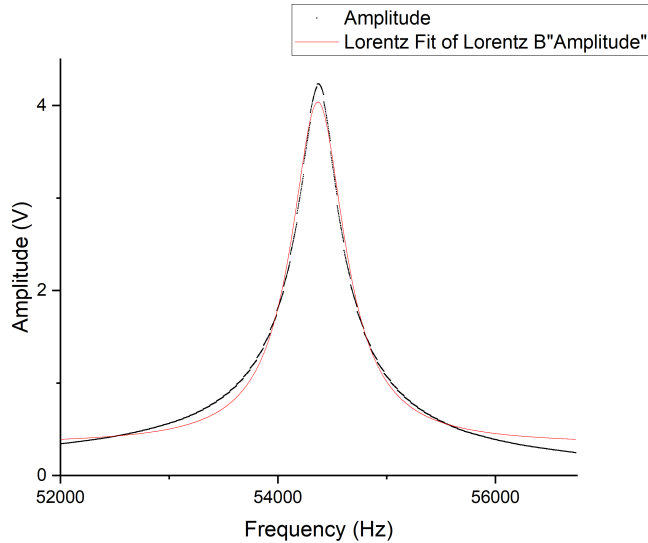


Figure 3

Where the resonant frequency is found to be 54368.8 ± 0.7 Hz.

5.1 Sample B

Sample B is gold on a flat layer of silicon. The gold is deposited to the silicon through mask evaporation of polystyrene spheres, then, the small gold islands are set on the silicon substrate. In the images, gold appears triangular in star patterns as the lighter contour whereas the polystyrene balls were where the darker hexagons are. From the images, a line is drawn and the sphere size is found. The found diameter of the polystyrene spheres is $1.91 \pm 0.02 \mu\text{m}$

In sample B, a good example of when the microscope scans too fast is seen in figure 5 and 6.

In Fig. the path of scanning is from left to right and in Fig. the path of scanning is from right to left.

In sample B, a good example of drift is shown between the front and back

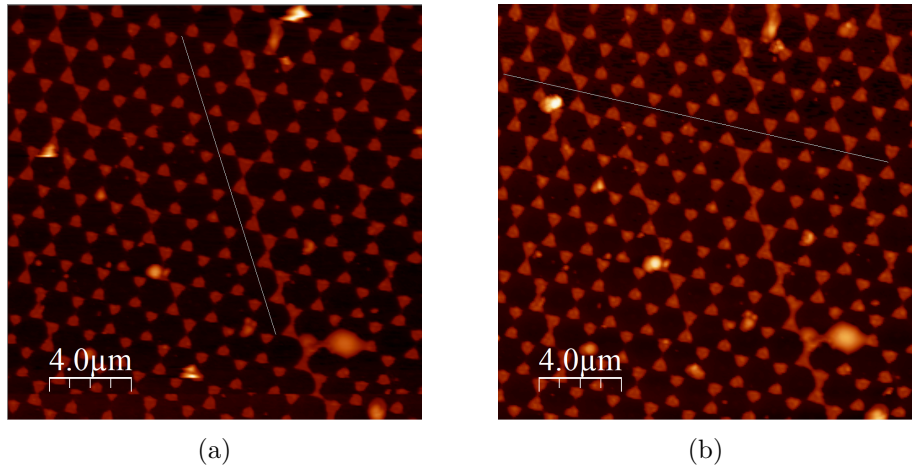


Figure 4

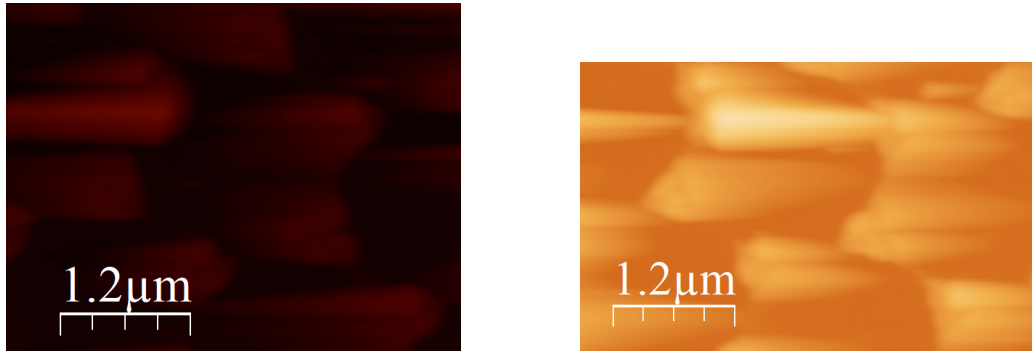


Figure 5

Figure 6

sweeps in figure 7. The front sweep is shifted negatively from the back sweep.

The front voltage is shifted to the right of the back voltage by 0.0008 ± 0.0005 V

In sample A, gold on graphite is seen in figure 8.

The brightly coloured spots on the right of the picture are contamination, likely from dust particles. The gold is the brighter contours and the graphite is the darker section.

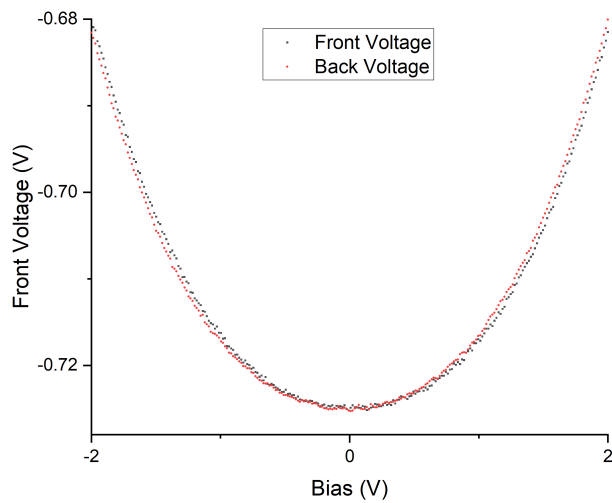


Figure 7

5.2 Work Function

The relative work functions of the tip with respect to graphite and the tip with respect to gold are the bias at the minimum of the respective graphs. Here, the bias at minimum is -0.01 ± 0.01 V for gold and 0.07 ± 0.01 V for graphite. The error is taken from the interval between x-axis points.

5.3 Tip Shape

To obtain measurements which would later allow us to determine the shape of the tip, we did a similar process to the other voltage spectroscopy, although this time it did not matter which material that the tip was over. We ramped the voltage from -9 V through to +9 V, and the tip was not fixed at a constant height, but allowed to move. We measured the tip height as a function of applied potential difference.

We performed this voltage spectroscopy twelve times at different points on the sample, over both gold and graphite.

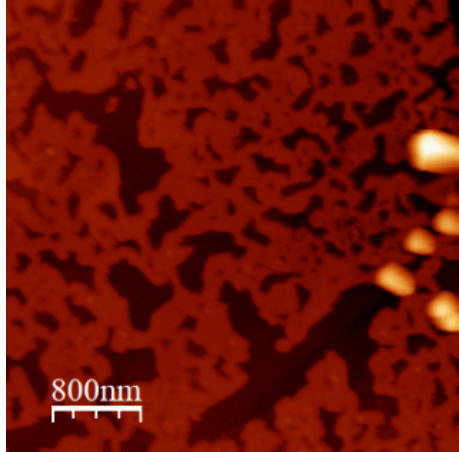


Figure 8

6 Analysis and discussion

6.1 Work Function

The work function of HOPG is quoted at 4.6 eV from a 2001 study[2] however another study quotes the work function as 4.65 eV [11], and another study in 2011 quotes the work function as < 4.75 eV[12]. The work function of gold is also difficult to determine. In a 1966 study, contaminated gold was quoted to have a work function of 4.68 ± 0.03 eV while the work function of pure gold was 5.28 ± 0.02 eV[1]. That is a range of 0.6 eV!

In this experiment, the relative work functions of the tip to graphite and the tip to gold are found. The difference between the two values yields the relative work function between gold and graphite: 0.08 ± 0.02 eV.

The value agrees with literature to a certain extent. Assuming the gold particles are on contaminated surfaces (the most likely source of contamination is water from the air) and taking the work function of graphite from the 2001 study, the results confirm the literature values. However, many factors affect work function, such as temperature, so these values are not appropriate for accurate numerical confirmation, rather they are in the same order of magnitude as current values.

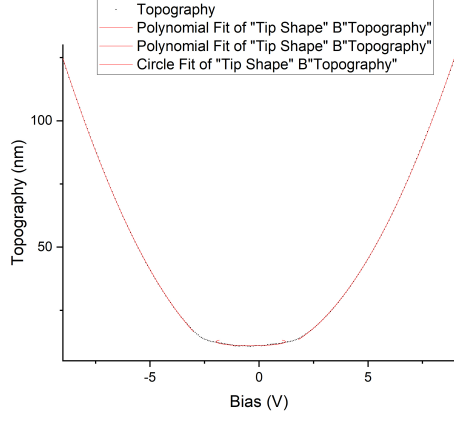


Figure 9

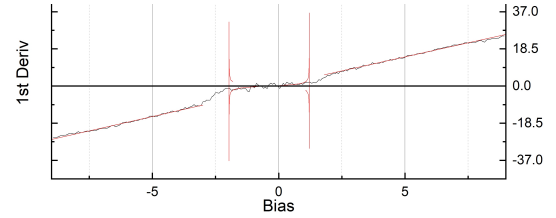


Figure 10

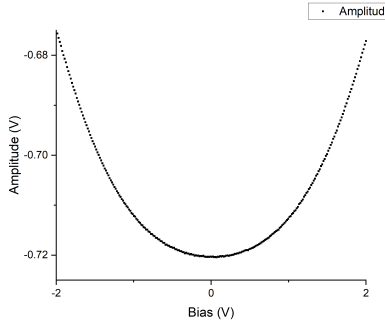


Figure 11: Tip Amplitude vs applied voltage bias on graphite

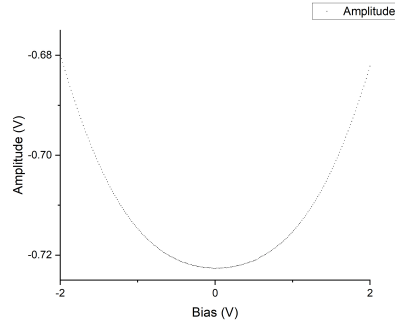


Figure 12: Tip Amplitude vs applied voltage bias on gold

6.2 Tip shape discussion

The tip shape is analysed by cycling the bias from -9 V to +9 V. Here, attractive forces from the chemical potential are seen in the region close to 0 V but the electrostatic force becomes dominant in the large magnitude regions. A circular fit is used in the graph where the derivative is close to zero, and a quadratic fit is used where the derivative is linear to show the error in the final values from the fit.

The circular fitting equation is:

$$(x - x_c)^2 + (y - y_c)^2 = r^2$$

Where the constants are found to be $x_c = -0.38 \pm 0.03$ V, $y_c = 12.56 \pm 0.06$ nm and $r_2 = 2.53 \pm 0.08$ nm V

The polynomial fitting equation is:

$$f(x) = ax^2 + bx + c$$

With the fitted values being:

$$\begin{aligned} a_{-ve} &= 1.430 \pm 0.008 & b_{-ve} &= -0.91 \pm 0.09 & c_{-ve} &= 0.9 \pm 0.3 \\ a_{+ve} &= 1.398 \pm 0.005 & b_{+ve} &= -0.52 \pm 0.05 & c_{+ve} &= 7.8 \pm 0.1 \end{aligned}$$

Using the equations found in Appendix 4 [20], a conical shape is found from the polynomial fits and a spherical shape is found from the circular fit.

6.2.1 Spherical Model

$$F = -\frac{\pi\epsilon_0 RU^2}{d} \quad (1)$$

$$F' = \frac{\pi\epsilon_0 RU^2}{d^2} \quad (2)$$

Where U is the applied voltage, d is tip to sample distance, R is the tip radius, F is tip force, F' is the tip force gradient.

To calculate the shape of the tip, we did not need the equation for the force 1, but only the force gradient, given in 2.

Taking the results of [16], the force gradient can be expressed as shown

$$\frac{\partial F_{\text{total}}}{\partial z} = k \left(\frac{1 - 2a^2 + \sqrt{4Q^2(a^2 - 1) + 1}}{2(Q^2 - a^2)} \right) \quad (3)$$

where $a = \frac{A_0}{A} = \frac{\text{amplitude of the free resonance}}{\text{feedback amplitude}}$ and Q is the *quality factor* of the cantilever.

$$a = -5.86 \pm 0.02 \quad (\text{dimensionless})$$

$$Q = 163.021 \pm 0.001 \quad (\text{dimensionless})$$

$$k = 1.19763 \pm 0.00001 \quad N/m$$

As all of these values are constants, we get an output once we have inputted all of the values and found the propagation of the error,

$$\frac{\partial F_{\text{total}}}{\partial z} = 0.0410 \pm 0.0003 Nm^{-1}$$

We can now equate this value to equation 2 to solve for the value of R . For the value of $(\frac{U}{d})^2$, we used the average of the values we recorded for U and d where they had a linear relationship with one another. This turns out to be the range $-9 < U < -3$ and $2 < U < 9$, measured in volts.

Thus, we found the radius of the tip for a spherical model to be $R = 118 \pm 0.9$ nm

6.2.2 Conical Model

The same paper also gives a way to model the tip as a cone.

$$F = -\frac{\alpha^2 U^2}{4\pi\epsilon_0} \ln\left(\frac{L}{4d}\right)$$

$$F' = \frac{\alpha^2 U^2}{4\pi\epsilon_0 d}$$

$$\alpha = \frac{2\pi\epsilon_0}{\arcsin\left(\frac{1}{\tan(\frac{\theta}{2})}\right)}$$

where θ is the full cone angle and L is the tip length.

By following the same process as we did before, we find that $\alpha = 60 \pm 9$ degrees.

6.3 Polystyrene spheres on Sample B

The usefulness of images (in terms of how well we can analyse them) depends on two conditions: magnitude of scanning speed and size of scanning area. When the scan is in appropriate states, more precisely, the speed is not too fast(smaller than 3 line/sec) and the size is not too large(smaller than $50\mu\text{m} \times 50\mu\text{m}$), we receive a plain pattern.

To measure the size of the (removed) polystyrene spheres, the scans of the sample yield the locations of the gold particles deposited between the spheres. Using the AFM imaging software we measure the difference between points on the sample. Instead of measuring the cross-section of one

sphere, we measure the distance across multiple spheres (along a line of the hexagonal packing symmetries), and then divide this distance by the number of traversed spheres to get a more accurate value.

The evaporated gold could have spread underneath the spheres and encroached on their shadow. Therefore, there is qualitative error associated with where to start measuring, since the gold deposits that are left are not necessarily perfectly aligned with where the spheres were.

As mentioned previously, the gold triangle vertices should be combined and then we their diameter measured precisely, but there are gaps in each observed image. When we measure the distance across multiple spheres, it might not cross the centre of each sphere. Another source of error is from the dimensions of the sample surface, the real sample surface is not like a xy-plane, it is in 3 dimensions instead of the images we captured.

6.4 Sources of Error

6.4.1 Hysteresis

Piezoelectric motors suffer from an effect known as hysteresis [14]. Hysteresis is a phenomenon whereby the state of a system depends on its prior states. In the case of a piezoelectric element, this means that applying a certain voltage, and then reducing the voltage back to 0, will leave the element at a new point, different to where it started from.

Hysteresis is a property of some materials, and is ultimately caused by the alignment of the spin of electrons in a material, and the retention of this electromagnetic alignment, after the applied force has been removed.

In our specific case, this results in the scans of the AFM taken in one direction, being different to those taken in the opposite direction. In order to reduce this problem, many AFM scanners, including ours, scan a sample in such a way so as to only record data while scanning in a certain direction¹.

However, although this problem can be reduced in the fast-scan direction (by separating the scans in the “positive” fast-scan direction from those in the “negative” fast-scan direction), it is not possible to do an analogous procedure in the z direction, since the tip needs to stay at a fixed distance to the sample.

¹more precisely, the data is recorded in both directions, but the data from the two directions are kept separately in different files

Thus the effect of hysteresis can only be accounted for to a certain extent.

6.4.2 Scanning Speed

Another source of inaccurate scanning is if the scanning speed of the tip is too fast. If the tip is scanning horizontally very fast, then the time needed to react to a change in height corresponds to a large horizontal distance. This results in the features of a sample being smeared across the image. See figures 5 and 6 for images we took at a high scanning speed.

7 Conclusion

Overall, the Atomic Force Microscope allows the user to take clear images at the nano scale. This report describes three different methods of the microscope (contact, non contact with feedback and non contact without feedback) and produces images for two different gold samples. Through this process, analysis on hysteresis, drift and other limitations of the microscope are explored and a value of the relative work function between gold and graphite is obtained. The value is 0.08 ± 0.02 eV which agrees with literature, but is limited in confirming the theory.

References

- [1] Riviere, J. C. "The work function of gold." *Applied Physics Letters* 8.7 (1966): 172-172.
- [2] Hansen, Wilford Hansen, Galen. (2001). Standard reference surfaces for work function measurements in air. *Surface Science*. 481. 172-184.
- [3] Binnig, G.; Rohrer, H. (1986). "Scanning tunneling microscopy". *IBM Journal of Research and Development*. 30 (4): 355–69.
- [4] "In 1986 Gerd Binnig and Heinrich Rohrer shared the Nobel Prize in Physics for inventing the scanning tunneling microscope"
- [5] Binnig, G.; Quate, C. F.; Gerber, C. (1986). "Atomic Force Microscope". *Physical Review Letters*. 56 (9): 930.
- [6] Butt, H; Cappella, B; Kappl, M (2005). "Force measurements with the atomic force microscope: Technique, interpretation and applications". *Surface Science Reports*. 59 (1): 1–152.
- [7] Morris, Victor J., Andrew R. Kirby, and A. Patrick Gunning. *Atomic force microscopy for biologists*. 1999.
- [8] Sugimoto, Yoshiaki, et al. "Chemical identification of individual surface atoms by atomic force microscopy." *Nature* 446.7131 (2007): 64.
- [9] Sarid, Dror, et al. "Scanning force microscopy-with applications to electric, magnetic and atomic forces." *Microscopy Microanalysis Microstructures* 2.6 (1991): 649-649.
- [10] Zur Mühlen, A., et al. "Atomic force microscopy studies of solid lipid nanoparticles." *Pharmaceutical research* 13.9 (1996): 1411-1416.
- [11] Schroeder, P. G., et al. "Investigation of band bending and charging phenomena in frontier orbital alignment measurements of para-quaterphenyl thin films grown on highly oriented pyrolytic graphite and SnS₂." *Surface science* 459.3 (2000): 349-364.
- [12] Shiraishi, Masashi, and Masafumi Ata. "Work function of carbon nanotubes." *MRS Online Proceedings Library Archive* 633 (2000).
- [13] Rugar, Daniel, and Paul Hansma. "Atomic force microscopy." *Physics today* 43.10 (1990): 23-30.

- [14] Lapshin, Rostislav V. "Analytical model for the approximation of hysteresis loop and its application to the scanning tunneling microscope." Review of Scientific Instruments 66.9 (1995): 4718-4730.
- [15] Rugar D, Hansma P. Atomic force microscopy[J]. Physics today, 1990, 43(10): 23-30.
- [16] Lü J, Guggisberg M, Lüthi R, et al. Surface potential studies using Kelvin force spectroscopy[J]. Applied Physics A: Materials Science Processing, 1998, 66: S273-S275.
- [17] Smit B. Phase diagrams of Lennard-Jones fluids[J]. The Journal of Chemical Physics, 1992, 96(11): 8639-8640. [interaction distance diagram] ThermoMicroscopes, "Basic guide to Scanning Probe Microscopy": 6 Fig 1-4
- [18] Olssen et al., J. Appl. Phys. 84, 8, 4060 (1998): 4060-4061
- [19] Howland, Rebecca, and Lisa Benatar. A Practical Guide: To Scanning Probe Microscopy. Park scientific instruments, 1996. page 9, figure 1-5.
- [20] Olsson, L., et al. "A method for in situ characterization of tip shape in ac-mode atomic force microscopy using electrostatic interaction." Journal of applied physics 84.8 (1998): 4060-4064.